The 9th International Supercritical CO_2 Energy Technologies Symposium
March 2 - 5, 2026, Pittsburgh, PA
Paper #028

Thermohydraulic performance of a supercritical CO_2 PCHE for heat pipe microreactors

Curtis H. Foster
PhD Student
University of Wisconsin
Madison, WI

Tiago A. Moreira
Assistant Professor
University of Campinas
Campinas, São Paulo

Gregory F. Nellis
Professor
University of Wisconsin
Madison, WI

Mark H. Anderson
Professor
University of Wisconsin
Madison, WI

Curtis Foster is a Graduate Research Assistant working at the University of Wisconsin-Madisons Solar Energy Laboratory and Thermal Hydraulics Laboratory. His research is in the development, analysis, and testing of heat pipe microreactor heat exchangers. He primarily focuses on modeling and testing compact heat exchangers in the context of air and sCO_2 Brayton cycles with the goal of developing advanced heat exchanger technologies for heat pipe microreactors.

Dr. Tiago Moreira is a professor in the Department of Energy at the School of Mechanical Engineering, University of Campinas (UNICAMP). He previously served as a Scientist I and a Postdoctoral Research Associate at the Solar Energy Laboratory of the University of Wisconsin-Madison. His research focuses on the thermal-hydraulics of nuclear reactors and high-temperature power generation advanced systems. He graduated in Mechanical Engineering by the University of Sao Paulo (USP), where he also obtained his Masters (research theme: heat transfer of nanofluids during single-phase flow and flow boiling in microchannels) and Ph.D. (analysis of the condensation of hydrocarbons and their mixtures inside horizontal channels applied to commercial and industrial refrigeration).

Professor Nellis has engaged in research that builds on his expertise in cryogenics, refrigeration, heat transfer, thermodynamics, and energy systems. Professor Nellis received the R.W. Boom Award in 2008 from the Cryogenic Society of America and was elected a Fellow of ASHRAE in 2013.He co-authored the second edition of the book Cryogenic Heat Transfer which is widely used in the industry. He has received "Distinguished Professor" awards from the engineering student organizations Polygon and Pi Tau Sigma several times. Professor Nellis, together with his colleague Professor Sanford Klein, have co-authored three undergraduate-level texts and a reference book.

Dr. Mark Anderson is a Professor in the Department of Mechanical Engineering, Associate Chair of Mechanical Engineering, Director of the University of Wisconsin's Thermal Hydraulic Laboratory, and has an affiliate appointment in Nuclear Engineering and a zero-time staff appointment at Idaho National Laboratory. He also manages the UW–Madison Tantalus facility in Stoughton, WI. Dr. Anderson studies the thermal-hydraulic performance and material-related issues of advanced energy systems with fluids such as salts, liquid metals, supercritical water, and supercritical carbon dioxide. He is also currently the U.S. representative to the International Atomic Energy Agency (IAEA) for the coordinated research project on supercritical fluids and has active research on advanced nuclear reactors, solar thermal energy, energy storage, and advanced fossil power generation. Dr. Anderson is a lifetime member of the American Nuclear Society (ANS) and a member of the American Society of Mechanical Engineers (ASME). He has been awarded over five patents and has published over 200 papers in various areas related to physics, energy science, production, and utilization.

ABSTRACT

Microreactors offer a promising solution for delivering clean, reliable power to remote communities, industrial sites, and military installations. Heat pipe cooled microreactors, in particular, provide inherent robustness and simplicity due to their lack of moving parts. Integration with high efficiency power cycles, such as supercritical carbon dioxide (sCO_2) Brayton cycles, require an effective primary heat exchanger between the heat pipe array and the working fluid. This study presents the design, fabrication, and experimental evaluation of a sub-sized printed circuit heat exchanger optimized for coupling a 5 MW(th) heat pipe microreactor to a recompression sCO_2 Brayton cycle. The test specimen, incorporating diffusion bonded stainless steel plates with etched microchannels, was instrumented with cartridge heaters and fiber optic temperature sensors and testing in the University of Wisconsin's $WisCO_2$ facility under inlet conditions up to 325°C, 10 MPa, and a mass flow rate of 0.16 kg/s. Thermohydraulic performance was assessed through pressure drop measurements, approach temperature, and high resolution solid temperature mapping. Results demonstrate the PCHE's capability to achieve efficient heat transfer and predictable pressure drops, providing future benchmark data for validating CFD models and informing full-scale heat exchanger designs. This work establishes a framework for future integration of heat pipe microreactor with high efficiency sCO_2 power cycles and supports DOE microreactor Program objectives for advanced reactor development.

INTRODUCTION

Microreactors have been proposed to replace diesel generators and provide carbon-free power for applications such as remote communities, industrial processes, military installations, and possible integration with microgrids [1]. These microreactors are small nuclear reactors sized to provide 1-50 MW(e) of power and are specifically designed to be transportable, self-regulating, and factory manufacturable. The U.S. Department of Energy is sponsoring research to advance microreactor technology through the Microreactor Program, which aims to develop the infrastructure needed for advanced technology development and demonstration [2]. Idaho National Laboratory has developed nonnuclear test facilities to demonstrate microreactor technologies and verify digital models [3]. INL's Demonstration Of Microreactor Experiments (DOME) test bed is an example of such a facility. Westinghouse's eVinci™ and Radiant's Kaleidos are two of the first microreactors that will be installed in the DOME test bed [4]. The design of the heat pipe cooled eVinci™ stands out because of its current level of development and its passive heat removal system.

Heat pipe cooled microreactors utilize a monolith with fuel and heat pipes interspersed, creating a "solid-state" core with a passive heat removal mechanism [5]. This enables a design with minimal moving parts and that is inherently robust, increasing reliability in comparison to forced convection active systems, e.g., light water reactors (LWRs). The eVinci™ will offer 5 MW(e) of power utilizing sodium heat pipes and an air Brayton power conversion system [6]. The air Brayton cycle has been the predominant cycle proposed in literature and by other companies for power conversion in their first-of-a-kind heat pipe microreactors. A supercritical carbon dioxide (sCO_2) Brayton cycle has been proposed to improve cycle efficiency of these microreactors for future generations. Although these heat pipes offer inherent safety and passive heat transfer out of the reactor core, the integration between the heat pipes and an end-user application (power conversion system) poses a significant challenge due to the densely packed heat pipe array, high temperatures, and risk of radioactivity release. Although extensive studies have focused on the microreactor core, heat pipes, and the overall heat pipe microreactor system [7], [8], [9], limited attention has been given to the primary heat exchanger, which serves as the interface between the heat pipes and the power generation cycle.

In this system, the primary heat exchanger, also referred to as the heat pipe interface heat exchanger (HPIHX), transfers heat from the condenser ends of the heat pipes to the end use application, e.g., a sCO_2 Brayton cycle. Two HPIHX configurations commonly considered for use in air Brayton cycles are the annular flow and the shell and tube designs. However, for sCO_2 power cycles, the printed circuit heat exchanger (PCHE) has emerged as a leading candidate technology [10]. PCHEs are constructed by diffusion bonding stacks of thin metal plates, each containing chemically etched microchannels that form the flow passages. Figure 1 shows how the PCHE would interface with the condenser end of the microreactor heat pipes.

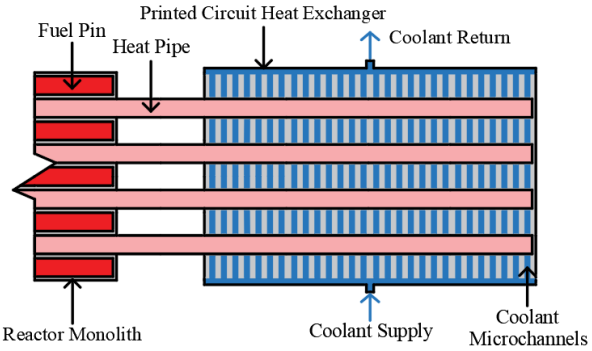

Figure 1. Diffusion bonded; printed circuit heat exchanger coupled to heat pipe microreactor.

PHCEs offer several advantages over the alterative designs [11]. Their microchannel architecture enables high heat transfer coefficients, large surface area to volume ratios, and minimal axial temperature gradients. A crossflow configuration promotes uniform heat transfer along the axial direction corresponding to the heat pipe condenser whereas the annular and shell and tube designs exhibit axial temperature variations that create non uniform boundary conditions for individual heat pipe condensers. Additionally, the maturity of diffusion bonded manufacturing processes contributes to reduced fabrication and assembly costs. PCHE technology is already well established in industry for applications involving high pressures and temperatures further supporting its suitability for microreactors.

Previously, a HPIHX design using the PCHE architecture was developed and modeled to optimize cycle performance for a sCO_2 recompression Brayton cycle paired to an “eVinci-like” heat pipe microreactor [12]. The recompression Brayton cycle was selected based on a comparison of various sCO_2 cycle layouts finding the recompression cycle to achieve the highest efficiency [13]. During the optimization process, the cycle model incorporated the primary heat exchanger model to predict both the pressure drop and approach temperature difference. The approach temperature is defined as the temperature difference between the maximum heat pipe condenser surface temperature and the bulk fluid outlet temperature, as expressed by:

$$\Delta T_{approach} = T_{hp,c} - T_{out} \quad (1)$$

This temperature difference, together with the heat pipe condenser temperature, can be used to estimate the maximum fluid outlet temperature and evaluate overall cycle performance. Building on these results, this paper presents the integration and experimental testing of the optimized PCHE design with the University of Wisconsin supercritical CO_2 ($WisCO_2$) test facility. A sub-sized PCHE test specimen was manufactured, instrumented, and fitted with cartridge heaters to simulate heat pipes. The $WisCO_2$ facility was adapted to meet heat exchanger inlet conditions of 500°C and 20 MPa, with a flow rate of 0.12 kg/s. Data was acquired at a pressure of 10 MPa and temperatures ranging from 75-325°C. Instrumentation included thermocouples and

differential pressure transmitters to provide thermal hydraulic performance metrics for future model validation. Additionally, the test specimen was fitted with fiber optic temperature sensors (FOTS), which enable high spatial resolution of the temperature distribution of the solid material. The objective of this work is to support advanced reactor development and address a critical gap in the literature by presenting experimental data from the first PCHE designed as a heat pipe interface heat exchanger for sCO_2 Brayton cycles.

RESULTS AND DISCUSSION

To carry out this experimental investigation, the following section describes the setup and testing of the PCHE prototype. Details are provided for the design and fabrication of the sub-sized test specimen, the configuration of the $WisCO_2$ test facility, and the procedures used for system integration and operation. The instrument layout, operating conditions, and data acquisition methods are outlined, followed by the presentation of key thermal and hydraulic performance results.

PCHE Test Specimen

In the PCHE configuration, the working fluid enters through a header positioned at the outer radius of the heat pipe array and exits through a central outlet header. The heat pipe array and heat exchanger are divided into six individual “wedges”. The sub-sized test specimen is taken as a subsection of an individual wedge and is shown in Figure 2.

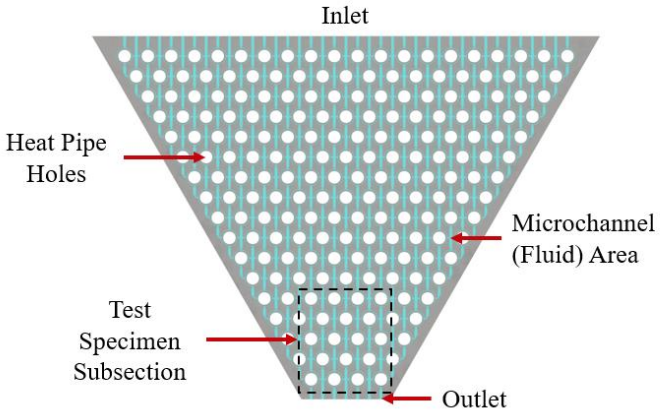

Figure 2. 1/12th wedge of heat pipe to working fluid PCHE, showing 102 heat pipe interface locations and the test specimen subsection.

The subsection was selected to match the microchannel outlet of the full-sized design and is shown as the dashed box, outlined in Figure 2. All key geometric parameters of the test specimen, including the heat pipe transverse and longitudinal pitch, microchannel dimensions, and heater interface wall thickness were identical to those of the full-scale design. The inlet temperature, pressure and mass flow rate were varied to reproduce similar operating conditions to those anticipated in the full-sized system. Cartridge heaters were employed to emulate the heat input from the reactor heat pipes, providing a comparable heat flux. The inlet conditions, flow rates and corresponding power densities (i.e., heat flux) for both the test specimen and full-scale PCHE are summarized in Table 1.

Table 1. PCHE test specimen geometry and experimental conditions.

Parameter	Test Specimen	Nominal HX
Inlet Temperature [ºC]	75, 200, 325	475
Outlet Temperature [ºC]	320-530	645
Inlet pressure [MPa]	10	20
Mass flux [kg/s-m^2]	270-1060	400-1590
Reynolds Number [-]	5200-28500	1000-6500
Power density [W/cm^2]	12.6	10.3

The test specimen consisted of a stack of diffusion-bonded 316/316L stainless steel plates, including sixteen chemically etched flow plates, one instrument plate, and two machined end plates forming the top and bottom of the stack. One of the etched flow plates also featured etched channels for pressure tap measurements within the microchannel. The material was supplied by CompRex LLC, which also coordinated the chemical etching and completed the diffusion bonding. Following fabrication, the specimen was sent to the University of Wisconsin-Madison, where a computed tomography (CT) scan was performed to evaluate the actual microchannel geometry of the test specimen, as is shown in Figure 3.

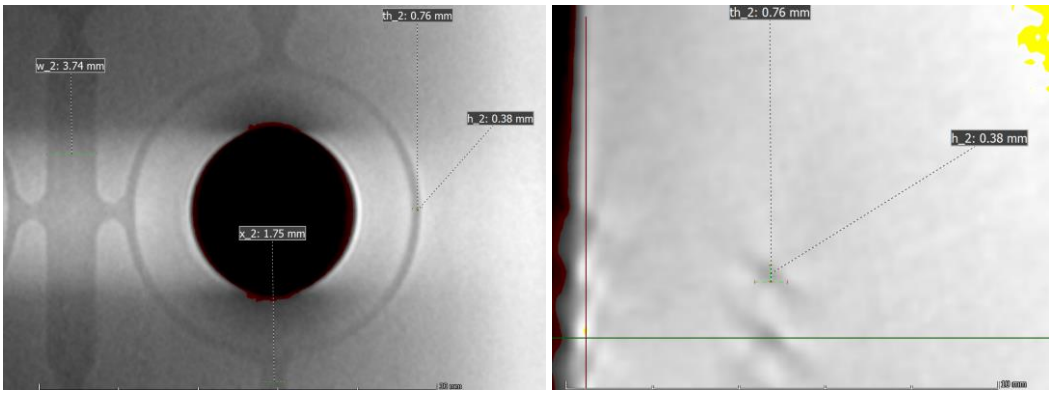

Figure 3. CT scan of test specimen with characteristic geometries dimensioned.

The dimensions identified in Figure 3 are summarized in Table 2, along with a comparison to the nominal design dimensions. The comparison indicates that the measured microchannels widths are approximately 0.25 mm smaller than the nominal values, corresponding to twice the difference in etch. The etch depth uncertainty is ±10% material thickness (0.15 mm), which accounts for the observed deviation in the channel geometry.

Table 2. PCHE test specimen geometry and experimental conditions.

Feature	Measurement [mm]	Nominal Design [mm]	Difference [mm]
Heater channel width (th_2)	0.76	1.0	0.24
Bypass channel width(w_2)	3.74	4.0	0.26
Throat width (x_2)	1.75	2.0	0.25
Etch depth (h_2)	0.38	0.5	0.12

Following the CT scan, cartridge heater holes were precision machined to a clearance of 25.4 µm. Instrumentation and process tubing were welded to the assembly prior to the installation of High Pressure Equipment (HiP) and Swagelok Co. fittings for the fluid connections. The test

specimen was then installed into a custom-fabricated insulation tray, which incorporated a high temperature calcium silicate block beneath the specimen and pourable microporous insulation surrounding and covering it. Figure 4 shows the test specimen within the insulation tray without the pourable insulation or cartridge heaters installed.

Figure 4. Test specimen positioned within the insulation tray after machining and installation of process connections.

Temperature measurements within the test specimen were obtained from the instrument layer, shown in Figure 5, which was diffusion-bonded between the fluid microchannel plates. Type-K thermocouple probes (OMEGA SCA3316-032G-6-SHX) were inserted into etched channels to record solid body temperatures, as illustrated in Figure 5. Stainless steel capillary tubes were embedded in straight channels across the instrument layer prior to diffusion bonding to accommodate the FOTS. Four thermocouple probes, labeled TC 1-4 in Figure 5, monitor the cartridge heater near wall temperatures. Based on flow direction, TC 3 and TC 4 correspond to the hottest region in the test specimen and, together with the bulk fluid outlet temperature, was used to determine the approach temperature.

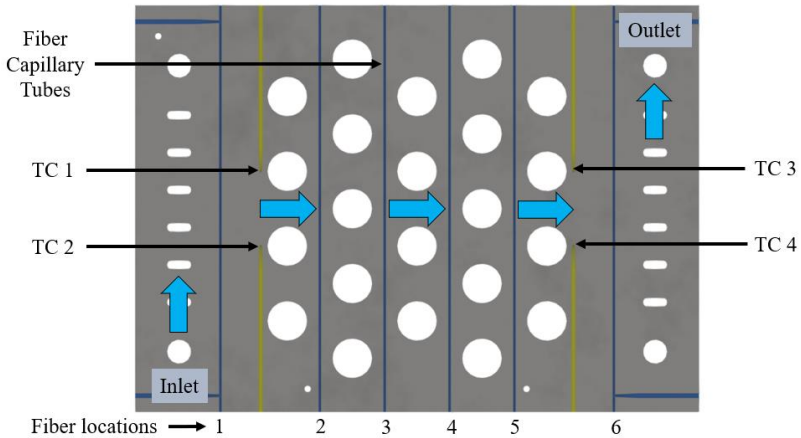

Figure 5. Test specimen instrument plate.

Pressure taps were located at the inlet and outlet headers as well as at the entrance and exit of the microchannel section. Pressure measurements were recorded using Yokogawa differential pressure transducers (Model EJA130E). Cartridge heaters, supplied by Watlow, were

installed in each heater bore using boron nitride paste to ensure good thermal contact. Each heater incorporated a center core Type-K thermocouple and had an outer diameter of 15.8 mm and a heated length of 25.4 mm, with a maximum power density of 12.6 W/cm^2. A fiber optic temperature sensor was constructed and installed in the test article. The sensor made six passes through the specimen, each routed through 0.41 mm in OD capillary tubing. These capillaries were enclosed within a series of larger tubes to allow the sensor to pass through the insulation tray and into the test specimen. A cross section of the capillary feedthroughs and the installed FOTS is shown in Figure 6.

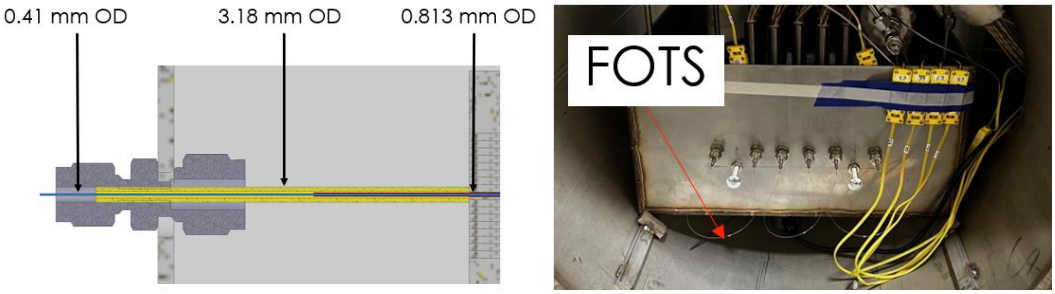

Figure 7. Insulated and instrumented test specimen and test apparatus.

Following the fabrication and instrumentation, the PCHE was installed in the WisCO$_2$ test facility. The subsequent section describes the test loop design, operating capabilities, and integration of the heat exchanger within the system.

Test Facility

The test specimen was installed into a custom test apparatus that provided biological shielding and access to the data acquisition hardware. The installed cartridge heaters and instrumentation can be seen in Figure 7, along with the insulated test specimen positioned within the apparatus.

Figure 7. Insulated and instrumented test specimen and test apparatus.

The test apparatus was subsequently integrated into the WisCO$_2$ test facility, as shown in Figure 8. The WisCO$_2$ loop includes a fixed displacement, triplex reciprocating pump and two diffusion-bonded heat exchangers. The primary purpose of the loop was to evaluate the thermal and

hydraulic performance of components coupled to the system, such as primary heat exchanger or office test sections. In this configuration, the PCHE test specimen served to emulate the coupling heat exchanger between the sCO_2 Brayton cycle and a heat pipe microreactor. The chiller, recuperator, and all interconnecting piping were designed to operate at supercritical pressures. A buffer volume was incorporated into the loop, serving two key functions: regulation of the overall system pressure and attenuation of pressure pulsation within the pump discharge piping. A Siemens Coriolis flow meter (Model MASSFLO 2100F D16) was installed downstream of the pump to measure the mass flow rate of carbon dioxide. Further details regarding the $WisCO_2$ facility design, operation, and component specifications are provided by Aakre et al. [14].

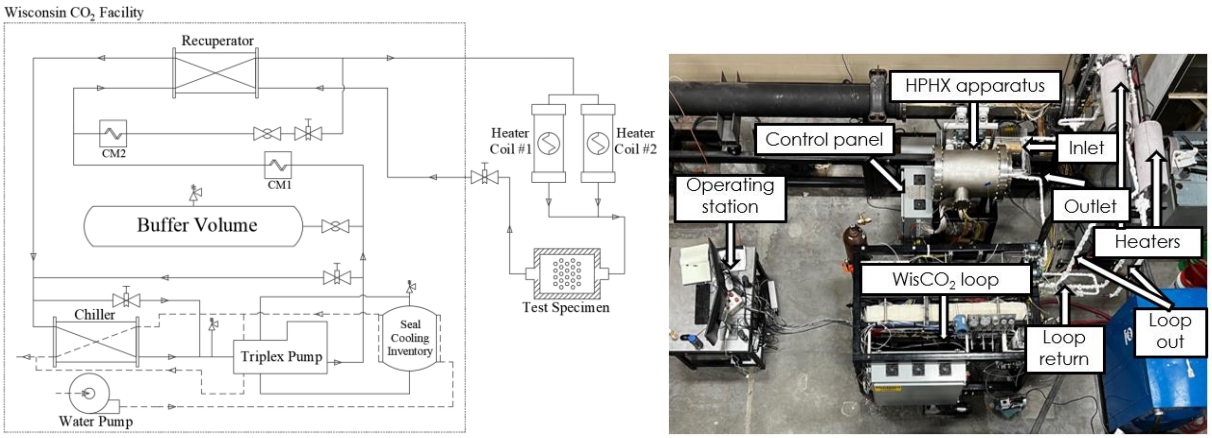

Figure 8. Line schematic (left) and overhead head image of $WisCO_2$ test facility.

After exiting the loop, the carbon dioxide stream was routed through two parallel direct electric resistance heaters, which provide additional heating and temperature control prior to entering the test specimen. Electrical current was applied directly to the tube containing the flowing carbon dioxide to achieve the desired inlet temperature. Downstream of the test specimen, a needle valve was used to regulate the outlet pressure and maintain the target loop operating conditions. System operation and data collection were managed using a LabVIEW™ interface connected to a national instruments CompactRIO (cRIO) control and data acquisition system equipped with modules 9213, 9214, and 9207 for continuous experimental data logging.

The $WisCO_2$ loop was first operated to reach the desired operating pressure and temperature for each test point. Next, the flow rate was set according to the target by adjusting the triplex pump frequency, return regulating valve, and a test section bypass valve. The heater power would be adjusted in parallel to achieve the desired temperature, pressure, and mass flow rate. Once steady state conditions were achieved, defined as temperature changes less than 0.2°C over 5 minutes, data was recorded for 90 s at a sample rate of 1 hz. The primary measurements recorded included the mass flow rate, $\dot{m}$, inlet pressure, P_{in}, total pressure drop ΔP_{total}, channel pressure drop, $\Delta P_{channel}$, inlet and outlet fluid temperature, T_{in} and T_{out}, temperature of the fiber, T_{fiber}, and two heater wall temperatures, T_{s3} and T_{s4}, where 3 and 4 correspond to the thermocouple probes depicted in Figure 5.

The uncertainties associated with the pressure and differential pressure measurements were determined through calibration procedures conducted against NIST traceable ISO 17025/2017 certified pressure transducers from Rosemount and Yokogawa, respectively. Similarly, the uncertainties of the thermocouples used to measure the fluid inlet, fluid outlet, and maximum solid temperatures were established through calibration against a NIST traceable ISO 17025/2017 certified platinum resistance thermometer (Fluke Corporation). For the remaining

thermocouples and the Coriolis flow meter, uncertainties were taken from manufacturer specifications. The uncertainties of derived parameters such as the approach temperature difference, were quantified using the sequential perturbation method described by Taylor and Kuyatt [15]. A summary of all experimental uncertainties is provided in Table 8.

Table 3. Experimental Uncertainties.

Parameter	Uncertainty
$\dot{m}$	0.3%
P_{in}	62 kPa
$P_{channel}$	62 kPa
ΔP_{total}	0.4 kPa
$\Delta P_{channel}$	0.4 kPa
$\mathrm{T_{in}}$	0.9ºC
T_{out}	0.9ºC
T_{S3}	1.1ºC
T_{S3}	1.0ºC
T_{S3}	1.4ºC
$\Delta T_{approach}$	1.3ºC

Test Results

Experimental testing was completed for mass flow rates ranging from 0.04 to 0.16 kg/s, corresponding to mass fluxes from 270 to 1060 kg/m^{2}s, inlet temperatures from 75 to 325°C, and an operating pressure of 10 MPa. As previously noted, the performance of the test specimen was assessed by examining the measured approach temperature and pressure drop across the microchannel. Figure 9 presents the approach temperature and pressure drop as a function of Reynolds number, with each marker type and color representing a different carbon dioxide inlet temperature. Figure 9 highlights that the pressure drop increases with increasing temperature, a result of the lower density and higher fluid velocity within the channels. In contrast, the trend for approach temperature with increasing temperature is less straightforward. Between 200 and 325°C, the approach temperature decreases, indicating enhanced heat transfer, largely due to the increase in thermal conductivity of both carbon dioxide and stainless steel. However, for temperatures between 75 to 200°C, heat transfer does not necessarily improve, particularly at higher Reynolds numbers. This behavior is attributed to the significant variation in carbon dioxide properties near the critical point, specifically, below 100°C. At an inlet temperature of 75°C, the specific heat of carbon dioxide is roughly twice its value at 200 and 325°C, which strongly influences the heat transfer performance. The relatively small uncertainty in the pressure drop and approach temperature measurements, compared to the magnitude of the observed variations across the test matrix, provides confidence that the measured trends in pressure drop represent true physical behavior rather than measurement noise.

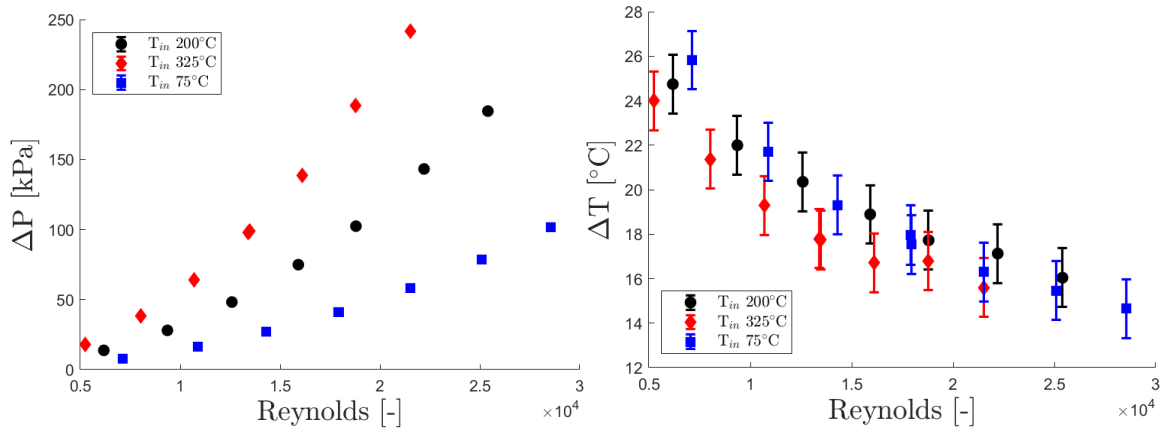

Figure 9. sCO2 test specimen testing results for channel pressure drop and approach temperature.

To estimate the heat losses of the test specimen. the measured electrical power was compared to the power transferred to the carbon dioxide, calculated as:

$$\dot{q}_{fluid} = \dot{m}_{hp}(i_{out} - i_{in}) \tag{2}$$

where $\dot{m}$ is the mass flow rate, and i_{in} and i_{out} are the specific enthalpies of carbon dioxide at the inlet and outlet, respectively. The specific enthalpies were determined from the measured temperatures and pressures at the corresponding locations. This analysis indicated an average heat loss of 220 ± 20 W, which corresponds to approximately 7% of the total electrical input power measured with a Fluke oscilloscope (Model 199C ScopeMeter). However, higher power losses were observed at lower flow rates, corresponding to higher system temperatures, relative to the higher flow rates.

A preliminary comparison between the experimental results and the CFD model is shown in Figure 10. The model predictions show strong agreement with the experimental data in capturing the trends of approach temperature and pressured drop across varying flow rates and temperatures. AT higher flow rates, the model tends to underpredict the pressure drop; however, this deviation may be influenced by uncertainties in the microchannel geometry. The approach temperature is also generally underpredicted by approximately 15%. Overall, the model provides sufficiently accurate predictions of the key thermal and hydraulic performance metrics required for the system level analysis.

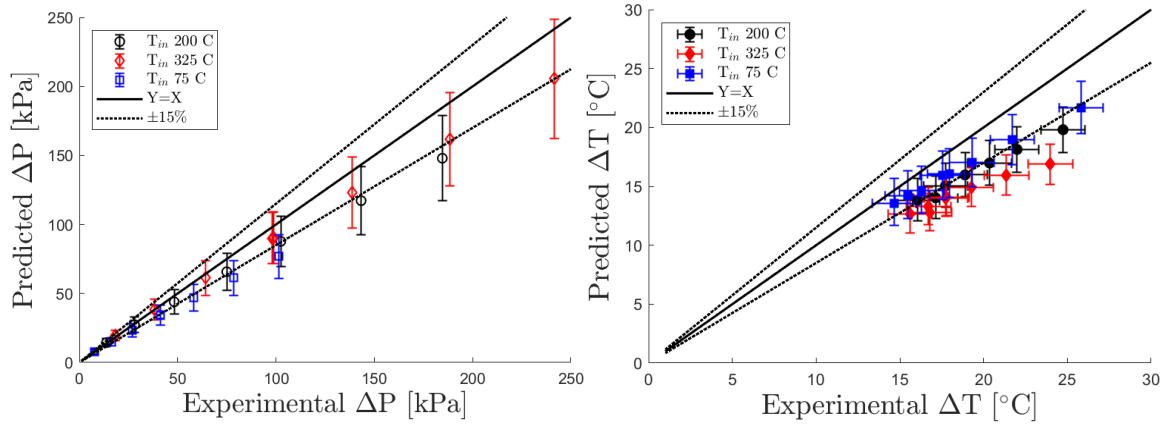

Figure 10. CFD predicted results versus experimental for pressure drop and approach temperature.

Temperature data obtained from the FOTS provide detailed insight into the temperature

distribution within the PCHE test specimen. Figure 11 presents transverse temperature profiles measured at the six locations shown previously in Figure 5, for an inlet temperature of 200°C and a mass flow rate of 0.16 kg/s. The right plot of Figure 11 offers a magnified view of the second FOTS pass through the heat exchanger, highlighting the localized thermal gradients across the specimen.

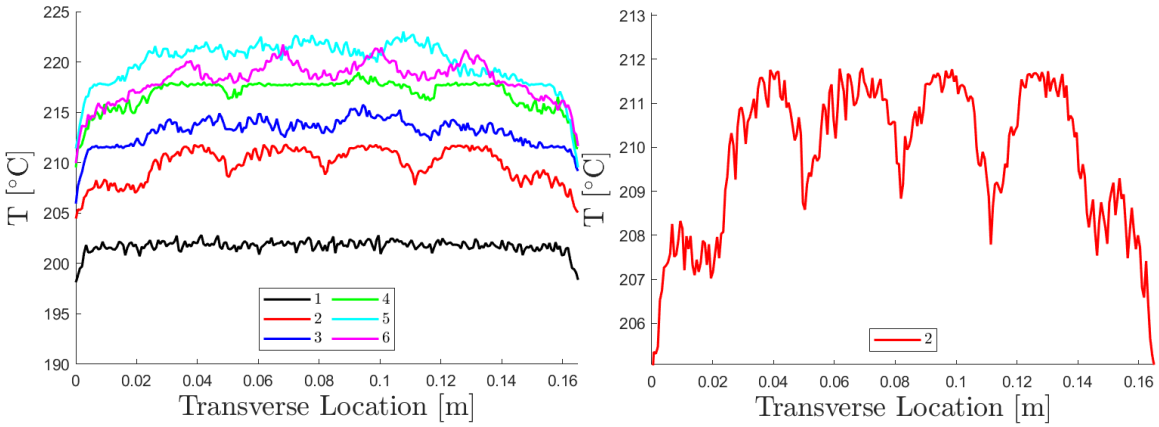

Figure 11. FOTS transverse temperature traces at six locations (left) and the second location (right).

The six temperature traces illustrate the evolution in the progression of the thermal field within the heat exchanger along the direction of fluid flow. The first trace corresponds to the region near the fluid inlet and shows a nearly uniform temperature close to the inlet condition of 200°C. The second trace provides greater detail into the temperature distribution within the heater array, revealing four distinct temperature peaks and five intervening dips that correspond to regions immediately downstream of the heaters and the cooler fluid channels approaching the subsequent heater row. This spatial variation is further depicted in Figure 12, where the fiber path is superimposed on the fluid microchannel layout. In the third through fifth traces, the overall temperature rises as additional heat is transferred from the heater array to the flowing carbon dioxide. The final trace exhibits a slight temperature decrease relative to the fifth, reflecting the approach of thermal equilibrium between the solid structure and the fluid near the heat exchanger outlet.

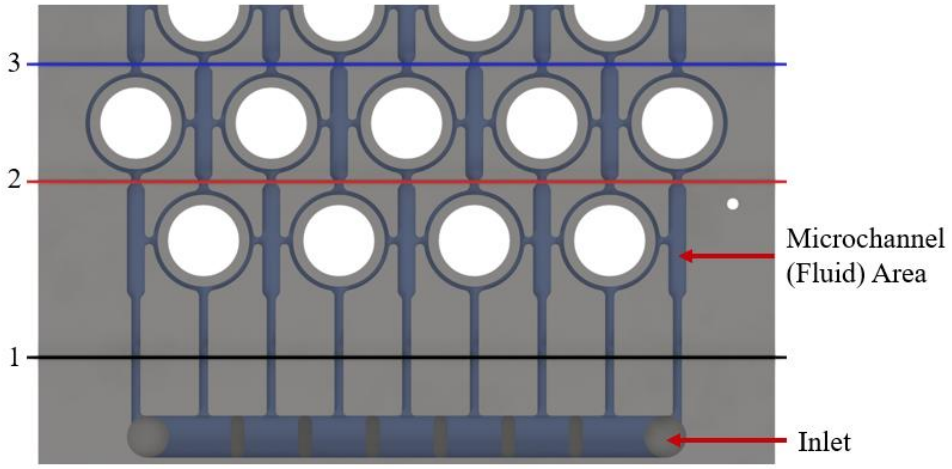

Figure 12. FOTS transverse temperature traces at location overlayed on fluid microchannel.

Conclusion

The present work presented the design, fabrication, and experimental evaluation of a printed circuit heat exchanger developed as a heat pipe interface heat exchanger for supercritical carbon dioxide Brayton cycle applications. A sub-sized test specimen was manufactured using diffusion bonding techniques and tested in the University of Wisconsin's WisCO_2 facility to assess its thermal and hydraulic performance under relevant operating conditions.

Testing was conducted at pressures up to 10 MPa, inlet temperatures ranging from 75 to 325°C, and mass fluxes between 270 and 1060 kg/m^2s. The measured pressure drop across the microchannel increased with temperature due to the combined effects of reduced fluid density and increased velocity, while the approach temperature exhibited non-monotonic tends linked to the strong property variations of carbon dioxide near the critical point. The fiber optic temperature sensor provided spatially resolved temperature measurements within the solid structure revealing local temperature gradients and heat transfer nonuniformities consistent with the heater array geometry.

A heat loss analysis indicated that external thermal losses were limited to approximately 7 % of the total input power, confirming that most of the supplied energy was transferred to the working fluid. The observed trends in pressure drop, heat transfer, and approach temperature provide valuable data for validating high fidelity numerical models of printed circuit heat exchangers for finding the thermal design of next generation HPIHX components for heat pipe microreactors. In summary the following conclusions were made from the present work:

- A sub-sized PCHE successfully operated under sCO_2 conditions up to 325°C and 10 MPa, demonstrating the structural and thermal integrity of the diffusion-bonded assembly.
- Measured pressure drop increased with temperature primarily due to density reduction and corresponding increases in velocity within the microchannels.
- Approach temperature behavior showed a complex dependence on inlet temperature, with enhanced heat transfer with increased temperature from 200 to 325°C but the was similar heat transfer similar performance from 75 to 200°C due to CO_2 property variations near the critical point.
- Fiberoptic temperature measurements provided high-resolution thermal mapping of the solid structure capturing heater induced nonuniformities and validating the manufacturing method for embedding the sensors.
- This study established a framework for future testing, including transient response characterization, model comparison, and failed heater scenarios.

Future work will focus on completing the comparison of the experimental data with model predictions to quantify the deviations, assessing performance at higher pressures and temperatures representative of full-scale reactor operation, and employing the embedded fiber optic sensor to capture transient and non-uniform temperature distributions during testing. These efforts will advance the understanding of thermal hydraulic behavior in compact diffusion bend heat exchangers and support the integration of heat pipe microreactors with high efficiency sCO_2 Brayton power systems. The experimental validation of the PCHE design directly supports the U.S. department of Energy's Microreactor Program objectives by advancing the understanding of heat transport system integration and providing the data necessary for accurate modeling of microreactor to Brayton cycle coupling.

REFERENCES

[1] D. Guillen *et al.*, “Development of a Non-Nuclear Microreactor Test Bed,” in *Transactions of the American Nuclear Society - Volume 121*, AMNS, 2019, pp. 1623–1626. doi: 10.13182/T30925.

[2] J. H. Jackson and P. Sabharwall, “Foreword: Special issue on the U.S. Department of Energy Microreactor Program,” *Nucl. Technol.*, vol. 209, no. sup1, pp. iii–v, Jan. 2023, doi: 10.1080/00295450.2022.2134723.

[3] P. Sabharwall *et al.*, “Nonnuclear Experimental Capabilities to Support Design, Development, and Demonstration of Microreactors,” *Nucl. Technol.*, vol. 209, no. sup1, pp. S41–S59, Jan. 2023, doi: 10.1080/00295450.2022.2043087.

[4] “3 Microreactor Experiments to Watch Starting in 2026,” Energy.gov. Accessed: Apr. 17, 2025. [Online]. Available: https://www.energy.gov/ne/articles/3-microreactor-experiments-watch-starting-2026

[5] B. H. Yan, C. Wang, and L. G. Li, “The technology of micro heat pipe cooled reactor: A review,” *Ann. Nucl. Energy*, vol. 135, p. 106948, Jan. 2020, doi: 10.1016/j.anucene.2019.106948.

[6] “eVinci™ Microreactor | Westinghouse Nuclear.” Accessed: Apr. 17, 2025. [Online]. Available: https://westinghousenuclear.com/energy-systems/evinci-microreactor/

[7] R. Hernandez, M. Todosow, and N. R. Brown, “Micro heat pipe nuclear reactor concepts: Analysis of fuel cycle performance and environmental impacts,” *Ann. Nucl. Energy*, vol. 126, pp. 419–426, Apr. 2019, doi: 10.1016/j.anucene.2018.11.050.

[8] I. Yilgor *et al.*, “Recent Developments and Findings of Heat Pipe Experiments for Microreactor Applications,” *Nucl. Technol.*, vol. 211, no. 5, pp. 905–939, May 2025, doi: 10.1080/00295450.2024.2375488.

[9] L. Ge *et al.*, “Improvement and Validation of the System Analysis Model and Code for Heat-Pipe-Cooled Microreactor,” *Energies*, vol. 15, no. 7, Art. no. 7, Jan. 2022, doi: 10.3390/en15072586.

[10] L. Chai and S. A. Tassou, “Performance Analysis of Heat Exchangers and Integrated Supercritical CO2 Brayton Cycle for Varying Heat Carrier, Cooling and Working Fluid Flow Rates,” *Heat Transf. Eng.*, vol. 44, no. 16–18, pp. 1498–1518, Oct. 2023, doi: 10.1080/01457632.2022.2140640.

[11] T. J. Morton, “IES Experimental Systems Development,” INL, 20–59847, 2020.

[12] C. Foster, M. Erickson, G. Nellis, and M. Anderson, “Optimal Microreactor Heat Pipe Heat Exchanger Microchannel Design for a Supercritical CO2 Brayton Cycle,” in *Transactions of the American Nuclear Society - Volume 131*, Orlando, FL. doi: doi.org/10.13182/T131-45859.

[13] M.-J. Li, H.-H. Zhu, J.-Q. Guo, K. Wang, and W.-Q. Tao, “The development technology and applications of supercritical CO2 power cycle in nuclear energy, solar energy and other energy industries,” *Appl. Therm. Eng.*, vol. 126, pp. 255–275, Nov. 2017, doi: 10.1016/j.applthermaleng.2017.07.173.

[14] S. R. Aakre, M. H. Anderson, and P. W. Brooks, “Volumetric efficiency and pressure pulsations of a triplex reciprocating supercritical CO2 pump,” *J. Supercrit. Fluids*, vol. 168, p. 105072, Feb. 2021, doi: 10.1016/j.supflu.2020.105072.

[15] B. N. Taylor and C. E. Kuyatt, *Guidelines for evaluating and expressing the uncertainty of NIST measurement results*, vol. 1297. US Department of Commerce, Technology Administration, National Institute of …, 1994. Accessed: Apr. 18, 2025. [Online]. Available: https://nvlpubs.nist.gov/nistpubs/Legacy/TN/nbstechnicalnote1297.pdf

ACKNOWLEDGEMENTS

This work was funded in part by the Department of Energy Office of Nuclear Energy's Nuclear Energy University Program under Award Number DE-NE0009141, along with support from the University of Wisconsin-Madison Thermal Hydraulics Laboratory. The views and opinions of authors expressed herein do not necessarily state or reflect those of the United States Government or any agency thereof. We would also like to give a special thanks to Paul Brooks from the UW-THL for his technical and mechanical support of the experimental apparatus.